九州大学大学院総合理工学報告
第32巻 第3号 12-18頁 平成22年11月

Engineering Sciences Reports, Kyushu University
Vol. 32, No. 3, pp. 12-18, NOV, 2010

Performance Investigation of a Novel CO_2 Compression-Adsorption Based Hybrid Cooling Cycle

Skander JRIBI *1,† Shigeru KOYAMA*1 Bidyut Baran SAHA*2
†E-mail of corresponding author: *s.jribi@cm.phase.kyushu-u.ac.jp*

(Received Nov. 01, 2010)

In this paper, the performance of a CO_2 based hybrid compression-adsorption cooling cycle is presented based on a transient mathematical model. In the proposed hybrid cycle two stage compression have been performed where CO_2 passes through the mechanical compressor at the low-pressure side. The compressed CO_2 from the mechanical compressor is then adsorbed in the designated adsorbers of the adsorption cycle. The chiller response as well as the chiller performance in terms of cooling capacity and coefficient of performance (COP) are investigated for different desorption pressures and gas cooler outlet temperatures. This novel hybrid cooling system attains similar cooling power and two to three folds COP values than those of the conventional CO_2 based vapor compression cycle with the same operating conditions. Therefore, the proposed system seems to be promising for automotive air-conditioning application where waste heat from engine is esteemed.

Key words: *COP, Cooling capacity, Activated carbon, CO_2, Hybrid, Chiller*

1. Introduction

Nowadays, R134a is the most used refrigerant in automotive and domestic air conditioning systems. However, the global warming potential (GWP) of R134a is as high as 1300. So it is essential to replace R134a with an environmentally benign refrigerant. CO_2 has the advantages of being natural, non-flammable and non-toxic refrigerant. Moreover, CO_2 has a zero ODP (Ozone Depletion Potential) and a negligible GWP equal to one. Recent studies show that CO_2 have similar performance to that of the R134a in automotive and domestic air conditioning applications.[1,2] However, CO_2 vapor compression cooling systems suffer from high working pressures which led to 10 to 30% higher manufacturing costs in comparing to those of the R134a based systems.[3] So, it is inevitable to improve the performance of CO_2 cooling systems.

In this study, a novel hybrid compression-adsorption cooling system is proposed where the compression process is realized in two steps: (i) mechanical compression at the low pressure side and (ii) thermal compression by adsorption/desorption processes at the high pressure side. This innovative hybrid system uses highly porous activated carbon of type Maxsorb III and CO_2 as the adsorbent-refrigerant pair. The paper also presents the transient mathematical model and the performance results of the hybrid cycle which are determined by cycle simulation.

2. Description of the Hybrid Cooling Cycle

Fig.1 shows the schematic diagram of the hybrid compression-adsorption cooling system which consists of: a gas cooler, a liquid reservoir, an expansion valve, an evaporator, a mechanical compressor and 4 adsorber/desorber beds filled with Maxsorb III. At first, the refrigerant, CO_2 is evaporated in the evaporator. Then, the evaporated refrigerant is compressed with the mechanical compressor and refrigerant pressure increases from P_{evap} to P_{comp}. After that, CO_2 is adsorbed in the beds assigned in adsorption mode known as adsorption process. Adsorption heat is generated during the adsorption process, which is removed by the cooling water. In the next step, the adsorber bed is disconnected from the mechanical compressor and it is heated by the hot water and this is known as

*1 Department of Energy and Environmental Engineering
*2 Department of Mechanical Engineering, Faculty of Engineering

pre-heating process. The pressure in the bed during the pre-heating process increases until it reaches the gas cooler pressure (P_{gc}). Concurrently, the valve between the bed and the gas cooler is opened and CO_2 starts to desorb from the desorbing bed. Desorption heat is absorbed during the desorption process, which is compensated by the heating water. The refrigerant desorbed from activated carbon is then cooled down in the gas cooler with the cooling water. Finally, CO_2 is expanded with the expansion valve.

As the process of adsorption/desorption is intermittent, four beds are employed to have a continuous cycle. The four beds works in different processes as shown in table 1. A, C, D and H denotes the processes of adsorption, pre-cooling, desorption and pre-heating, respectively. For example, in mode ADDA, beds 1,4 are in adsorption phase and beds 2,3 are in desorption phase. In mode ACDH, beds 1, 2, 3 and 4 are in adsorption, pre-cooling, desorption and pre-heating phases, respectively.

3. Mathematical Model

3.1 Adsorption isotherms

The equilibrium amount adsorbed of CO_2 onto Maxsorb III had been investigated experimentally[4] and Tòth equation (eq. 1) is used to correlate the adsorption data.

$$C = C_0 \frac{b_0 P \exp\left(\frac{Q}{RT}\right)}{\left(1+\left(b_0 P \exp\left(\frac{Q}{RT}\right)\right)^t\right)^{\frac{1}{t}}} \quad (1)$$

3.2 Heat of adsorption

The heat of adsorption is computed from the Clausius-Clapeyron equation given by:

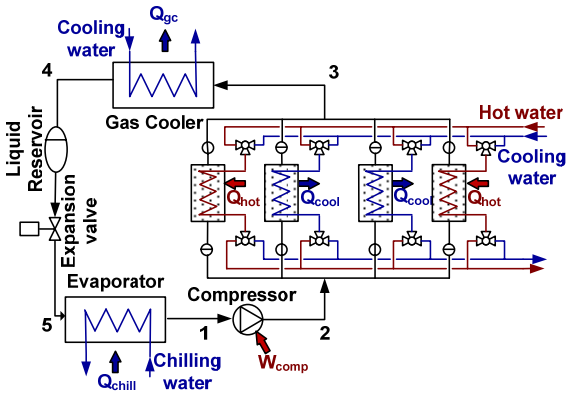

Fig.1 Schematic diagram of vapor compression-adsorption hybrid cooling system. Beds 1,4 are in desorption phase and beds 2,3 are in adsorption phase.

$$Q_{st} = RT^2 \left(\frac{\partial \ln P}{\partial T}\right)_C \quad (2)$$

The heat of adsorption derived from Tòth isotherm equation is constant and equals the parameter Q of eq. 1.

3.3 Adsorption kinetics

The adsorption rate is described by the linear driving force theory given by:

$$\frac{dc}{dt} = k_s a_v (C - c) \quad (3)$$

where C is the equilibrium uptake, c stands for instantaneous uptake and $k_s a_v$ is the overall mass transfer coefficient estimated experimentally for the adsorption of CO_2 onto activated carbon beads.[5]

$$k_s a_v = \exp\left(-\frac{1915}{T} + 1.776\right) \quad (4)$$

3.4 Adsorbing bed energy balance

The rate of change of adsorbing bed internal

Table 1 Modes of adsorption/desorption processes

Mode	ADDA	ACDH	AADD	HACD	DAAD	DHAC	DDAA	CDHA
Bed1	Adsorption			Pre-Heating	Desorption			Pre-Cooling
Bed2	Des.	Pre-Cooling	Adsorption			Pre-Heating	Desorption	
Bed3	Desorption			Pre-Cooling	Adsorption			Pre-Heating
Bed4	Ads.	Pre-Heating	Desorption			Pre-Cooling	Adsorption	

energy is equal to the heat released by adsorption process Q_{ads} minus the heat removed by the cooling water Q_{cool} and this is written as:

$$(Mc_p)_{bed}\frac{dT_{bed,ads}}{dt}=M_{MX3}\frac{dc_{ads}}{dt}\cdot \left(Q_{st}+h_{bed,ads}-h_{comp,out}\right)-(\dot{m}c_p)_{cool}(T_{cool,out}-T_{cool,in}) \quad (5)$$

where the cooling water outlet temperature is modeled by the log mean temperature difference (LMTD) method and expressed by:

$$T_{cool,out}=T_{bed,ads}+\left(T_{cool,in}-T_{bed,ads}\right)\exp\left(\frac{-UA_{bed}}{\left(\dot{m}c_p\right)_{cool}}\right) \quad (6)$$

3.5 Desorbing bed energy balance

The rate of change of desorbing bed internal energy is equal to the heat absorbed by desorption process Q_{des} minus the heat added by the heating water Q_{hot} and this is expressed as:

$$(Mc_p)_{bed}\frac{dT_{bed,des}}{dt}=M_{MX3}\frac{dc_{des}}{dt}Q_{st}-(\dot{m}c_p)_{hot}(T_{hot,in}-T_{hot,out}) \quad (7)$$

where the hot water outlet temperature is determined by:

$$T_{hot,out}=T_{bed,des}+\left(T_{hot,in}-T_{bed,des}\right)\exp\left(\frac{-UA_{bed}}{\left(\dot{m}c_p\right)_{hot}}\right) \quad (8)$$

3.6 Evaporator energy balance

The change of evaporator's internal energy is described by eq. 9. The first term in the right hand side (R.H.S.) of eq. 9 represents the latent heat of evaporation of the liquid refrigerant and the second term in the R.H.S. of eq. 9 represents the cooling capacity Q_{chill}.

$$(Mc_p)_{evap}\frac{dT_{evap}}{dt}=M_{MX3}\frac{dc_{ads}}{dt}\left(h_{evap,out}-h_{evap,in}\right)-(\dot{m}c_p)_{chill}(T_{chill,out}-T_{chill,in}) \quad (9)$$

The chilled water outlet temperature is given by:

$$T_{chill,out}=T_{evap}+\left(T_{chill,out}-T_{evap}\right)\exp\left(\frac{-UA_{evap}}{\left(\dot{m}c_p\right)_{chill}}\right) \quad (10)$$

The evaporator's overall heat transfer coefficient (UA_{evap}) is estimated for an average flow boiling heat transfer of CO_2 in round-tube.[6)]

3.7 Gas cooler energy balance

The change of gas cooler internal energy is equal to the heat removed from the desorbed refrigerant minus the heat released to the cooling water Q_{cw} and this is given by:

$$(Mc_p)_{gc}\frac{dT_{gc}}{dt}=M_{MX3}\frac{dc_{des}}{dt}\left(\left(h_{bed,des}-h_{gc}\right)\right)-(\dot{m}c_p)_{cw}(T_{cw,out}-T_{cw,in}) \quad (11)$$

where the cooling water outlet temperature from gas cooler is given by:

$$T_{cw,out}=T_{gc}+\left(T_{cw,in}-T_{gc}\right)\exp\left(\frac{-UA_{gc}}{\left(\dot{m}c_p\right)_{cw}}\right) \quad (12)$$

The gas cooler's overall heat transfer coefficient (UA_{gc}) is estimated for an average forced convection cooling heat transfer of CO_2 in microchannel tube.[6)]

3.8 Compressor energy balance

The mechanical work consumed by the compressor is expressed by:

$$\dot{W}_{Comp}=M_{MX3}\frac{dc_{ads}}{dt}\left(h_{comp,out}-h_{comp,in}\right) \quad (13)$$

An isentropic efficiency (η_{is}) of the compressor is assumed to be 0.8.

3.9 Mass balance

The mass balance implies that the adsorbed amount in the activated carbon is equal to the mass desorbed:

$$m_{ads}=m_{des} \quad (14)$$

where the masses adsorbed and desorbed are given by the following equations, respectively.

$$\frac{dm_{ads}}{dt}=M_{MX3}\frac{dc_{ads}}{dt} \quad (15)$$

$$\frac{dm_{des}}{dt}=M_{MX3}\frac{dc_{des}}{dt} \quad (16)$$

3.10 Energy balance

The energy balance (eq. 17) implies that the heats adsorbed by evaporator and desorption beds and the mechanical power consumed by compressor are equal to the heats rejected by

condenser and adsorption beds and this is written as:

$$Q_{chill} + Q_{des} + W_{comp} = Q_{gc} + Q_{ads} \quad (17)$$

3.11 System Performance

After achieving a cyclic-steady-state, the system performance is calculated for one complete cycle time that is: adsorption time + pre-heating time + desorption time + pre-cooling time. The average chilling capacity and COP during one cycle are expressed by eqs. 18 and 19, respectively.

$$Q_{chill} = \frac{\int_0^{t_{cycle}} (\dot{m}c_p)_{chill} (T_{chill,in} - T_{chill,out}) dt}{t_{cycle}} \quad (18)$$

$$COP = \frac{Q_{chill}}{W_{comp}} \quad (19)$$

4. Simulation Procedure

The simulation of the CO_2 based hybrid compression-adsorption cooling cycle transient mathematical model is carried out with the programming language Matlab. The differential equations are solved numerically with the function ODE45 and the thermophysical properties of the refrigerant are obtained by calling the Refprop routines of NIST software. The program starts with the initialization of isotherm parameters and heat exchangers constants (overall heat transfer coefficients, heating capacities,…)) and these are furnished in table 2. Then, the program initializes the variables of the system (inlet temperatures, adsorbing/desorbing time, desorbing pressure,…). After that, the program estimates the initial values of the differential equations parameters (T_{evap}, T_{cond}, $T_{bed1,...,4}$, $c_{1,...,4}$). As shown in table 1, there are 8 modes during one cycle time. The differential equations of each mode (energy balances and kinetic equations) are put together in a function called by the main program. The last results of the solved function are inputted as initial values to the next mode's differential equations. The key system variables are constantly computed and updated by numerical integration with time.

5. Results and Discussion

The temperature profiles of the different heat exchangers (gas cooler, evaporator and adsorber/desorber beds) are shown in Fig. 2. The inlet temperatures of hot, cooling and chilled waters are taken as 85, 30 and 15 °C, respectively. The adsorption and desorption processes time are fixed to 600 s and the switching time for pre-cooling and pre-heating phases is set automatically to the time at which the pressure in the heated bed becomes equal to the gas cooler pressure. It is found that the compression-adsorption hybrid chiller achieves cyclic steady-state operation within 3 cycle-times. From Fig. 2, it is noticed that the evaporator temperature is fluctuating due to the intermittent working of the thermal compression process. Its average value is equal to 9.7 °C for a chilled water inlet temperature of 15 °C. Moreover, the evaporator temperature increases of about 2 °C during switching time, that is one bed switch from adsorbing process to pre-heating process.

The outlet temperatures of chilled, cooling, and hot water as well as the compressor outlet

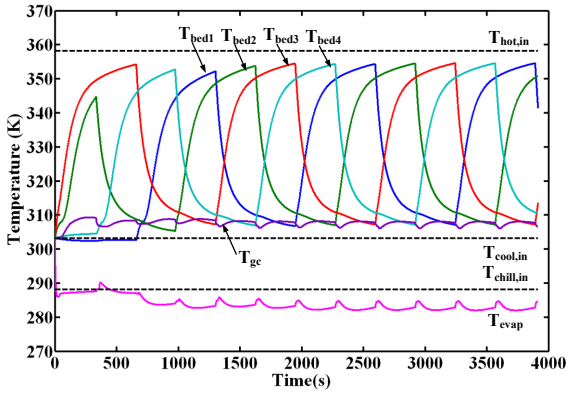

Fig.2 Temperatures change of evaporator, gas cooler and the 4 beds of the simulated cycle.

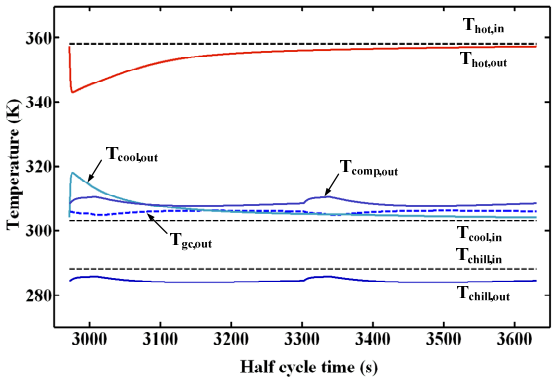

Fig.3 Outlet temperature profiles during half cycle time.

temperature are presented in Fig. 3. It is found that the cycle average chilled water outlet temperature is 12.4 °C for a chilled water flow rate of 0.2 kg·s^{-1}. The temperature approach between the water inlet temperatures and water outlet temperatures, at the end of adsorption and desorption processes, are found to be 0.65 and 0.9 °C for hot and cooling sources, respectively.

Fig. 4 denotes the *P-T-W* (Pressure-Temperature-Uptake) diagram of the simulated thermal compression process. From this figure, it is demonstrated that the hypothesis assumed in the mathematical model are validated. In fact, the desorption phase is realized at constant gas cooler pressure and the adsorption phase pressure follows the saturation pressure dictated by the evaporator's temperature. The pre-cooling and pre-heating phases are isosteric (parallel to dashed lines).

The *P-h* diagram of the hybrid system illustrates the energy saving by the thermal compression comparing to CO_2 conventional vapor compression cooling system (Fig. 5). It can be noticed that the gas cooler pressure and the gas cooler outlet temperature (point 4 in *P-h* diagram) will have a big impact on the performance of the system. In fact, these two key parameters dictate the amount of refrigerant being evaporated. This is illustrated in Figs. 6 and 7 which show the change of cooling capacity (CC) and COP for different gas cooler pressures (P_{gc}) and for refrigerant outlet temperatures from gas cooler ($T_{gc,out}$) of 35 and 40 °C. Moreover, the performance of the CO_2 based hybrid cycle (cycle 1-2-3-4-5) are compared to the conventional CO_2 vapor compression cycle (cycle 1-2'-4-5) for the same evaporation temperature of 10 °C.

The specific cooling capacity ($q_{evap} = h_1 - h_5$) of the hybrid system is similar to that of the conventional vapor compression system (dashed lines of Fig. 6). It increases with the increase of P_{gc} as the fraction of liquid refrigerant being expanded is higher. However, the refrigerant flow rate of the hybrid cycle decreases with higher desorption pressures as the amount desorbed decreases. This affects the CC of the hybrid system which attains a maximum value above which the added capacity no longer compensates the decrease in refrigerant flow rate. The optimal cooling capacity values, 2.34 and 1.68 kW, are attained at desorption pressures of 9.25 and 9.75 MPa for $T_{gc,out}$ of 35 and 40 °C, respectively.

Table 2 Constants parameters of the cycle

Symbols	Value	Unit
Adsorption isotherms constants		
C_0	3.05	kg·kg^{-1}
b_0	0.11	kPa^{-1}
Q	20.5	kJ·mol^{-1}
t	0.663	-
System design constants		
M_{MX3}/bed	20	kg
$(\dot{m}c_p)$	2926	W K^{-1}
$(\dot{m}c_p)$	836	W K^{-1}
$(Mc_p)_{bed}$	42100	J K^{-1}
$(Mc_p)_{gc}$	2484	J K^{-1}
$(Mc_p)_{evap}$	2484	J K^{-1}
UA_{bed}	1050	W K^{-1}
UA_{gc}	742	W K^{-1}
UA_{evap}	850	W K^{-1}

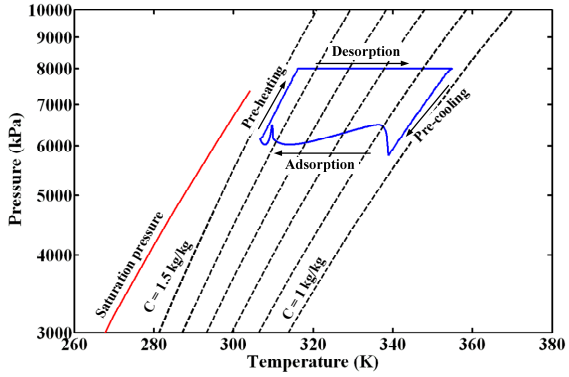

Fig.4 *P-T-W* diagram of Maxsorb III-CO_2 thermal compression process.

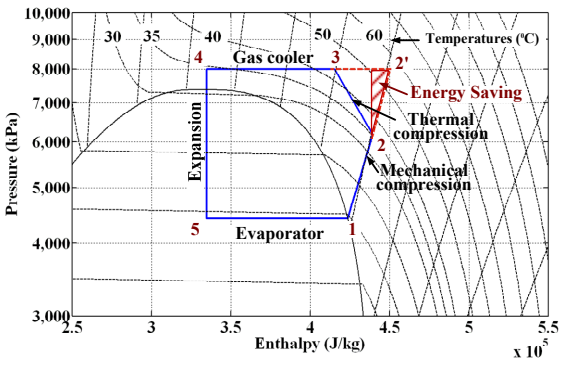

Fig.5 P-h diagram of CO_2 based hybrid cooling cycle.

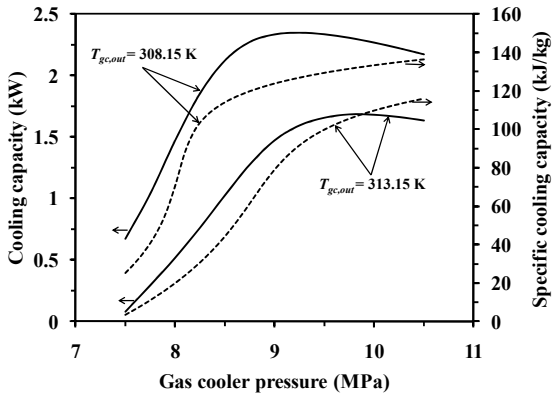

Fig.6 Specific cooling capacity (dashed lines) and cooling capacity (lines) of the hybrid cycle.

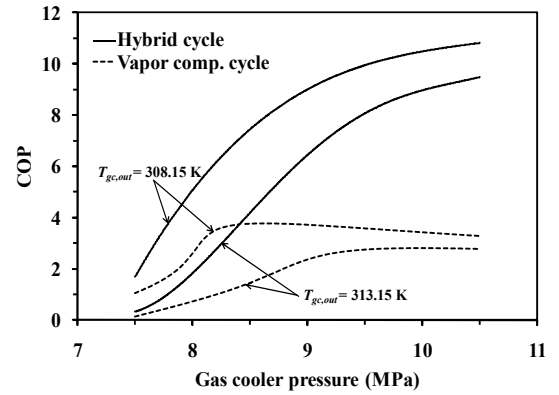

Fig.7 Comparison of COP of hybrid cycle (lines) and vapor compression cycle (dashed line).

The COP rises with the increase of discharge pressure and attains two to three times higher values comparing to that of the vapor compression cycle (Fig. 7). As explained above, the refrigerant flow rate of the hybrid cycle decreases for higher desorption pressures and therefore the compressor work also decreases. At the optimum CC reached, that is 2.34 and 1.68 kW for $T_{gc,out}$ of 35 and 40 °C, the COP attains 9.5 and 8.6, respectively.

6. Conclusions

An innovative environmentally benign as well as high performance hybrid cooling system is presented. The system uses CO_2 as the refrigerant and two steps compression; mechanical compression at the low pressure side and thermal compression employing adsorption/desorption processes in the high pressure side. In this system, the waste heat from automobile engine is utilized to power the thermal compression cycle. The analyses presented herein are based on the experimentally confirmed adsorption isotherm, adsorption kinetics, heat transfer coefficients and refrigerant property routines. This novel compression-adsorption system achieves 2 to 3 times higher COP comparing to that of the conventional vapor-compression systems and is suitable for automobile air-conditioning applications.

Nomenclature

$\dot{m}$	Mass flow rate (kg s^{-1})
A	Area (m^2)
b_0	Affinity at infinite temperature (Pa-1)
C	Adsorbed amount (kg kg^{-1})
c	Instantaneous uptake (kg kg^{-1})
C_0	Maximum uptake (kg kg^{-1})
CC	Cooling capacity (kW)
COP	Coefficient of performance (-)
c_p	Specific heat capacity (J kg^{-1} K^{-1})
h	Enthalpy (J·kg-1)
$k_s a_v$	Overall mass transfer coefficient (s^{-1})
M,m	Mass (kg)
P	Pressure (Pa)
Q	Heat (W); Heat of adsorption (J kg^{-1})
Q_{st}	Heat of adsorption (J kg^{-1})
R	Gas constant (J kg^{-1} K^{-1})
T	Temperature (K)
t	Heterogeneity factor (-), time (s)
U	Overall heat transfer coefficient (W m^2 K^{-1})
W	Work (W)

Subscripts

ads	Adsorption
bed	Sorption heat exchanger
chill	Chilled water
comp	Compressor
cool	Cooling water
cw	Cooling water of gas cooler
cycle	Cycle time (s)
des	Desorption
evap	Evaporator
gc	Gas cooler
hot	Hot water
in	Inlet
MX3	Maxsorb III
out	Outlet

References

1) Kim, M.-H., Pettersen, J., and Bullard, C.W., "Fundamental process and system design issues in CO_2 vapor compression systems", Progress in Energy and Combustion Science, Vol.30 (2004), pp.119-174.
2) Groll, E.A., and Kim, J.-H., "Review of recent advances toward transcritical CO_2 cycle technology", HVAC and R Research, Vol.13 (2007), pp.499-520.
3) Hrnjak, P., "Thermodynamic possibilities and technological opportunities for improving the science of refrigeration in search for low global warming thermal systems", Proc. Int. Symp. On Next-Generation Air Conditioning and Refrigeration Technology, Tokyo (2010), K09.

4) Jribi, S., El-Sharkawy, I.I., Koyama, S., Saha, B.B., “Study on activated carbon-CO_2 pair: adsorption characteristics and cycle performance”, Proc. Int. Symp. On Next-Generation Air Conditioning and Refrigeration Technology, Tokyo (2010), P19.
5) Shen, C., Grande, C.A., Li, P., Yu, J., and Rodrigues, A.E., “Adsorption equilibria and kinetics of CO_2 and N_2 on activated carbon beads”, Chem. Eng. J., Vol.160 (2010), pp.398-407.
6) Pettersen, J., Hafner, A., Skaugen, G., and Rekstad, H., “Development of compact heat exchangers for CO_2 air-conditioning systems”, Int. J. Refrigeration, Vol.21 (1998), pp.180-193.